# Improved nonvolatile holographic storage sensitivity of near-stoichiometric LiNbO$_3$:Fe:Mn crystals

**Xiaochun Li (李晓春)**[*], **Dengxue Qu (屈登学), Wenjie Wang (王文杰),**

**Xuejiao Zhao (赵雪娇), Lingling Zhang (张玲玲), and Xuejuan Meng (孟雪娟)**

*College of Physics and Optoelectronics, Taiyuan University of Technology, Taiyuan 030024, China*

[*]*Corresponding author: lixiaochun@tyut.edu.cn*

We investigate the nonvolatile holographic storage characteristics of near-stoichiometric LiNbO$_3$:Fe:Mn crystals with different Li$_2$O contents. Experimental results indicate that the optimal value of Li$_2$O content is about 49.6 mol%. Nonvolatile sensitivity $S'$ considerably improved to 0.15 cm/J because of the use of near-stoichiometric LiNbO$_3$:Fe:Mn with 49.6 mol% Li$_2$O.

*OCIS codes:* 210.2860, 190.5330, 090.7330, 160.5320, 160.3730.

*doi: 10.3788/COL201210.122101.*

Holographic data storage is a promising next-generation optical data storage technology because of its huge data capacity and fast data transfer rates; it is poised to change the way data written and retrieved[1]. Among various holographic storage materials, lithium niobate (LiNbO$_3$, LN) single crystals have been touted as potential storage materials for next-generation volume holographic memory because they are easily grown, low cost, and excellent photoelectric performance[2,3]. Two major issues, namely, volatility and low recoding sensitivity, currently impede the development of volume holographic memory. Several techniques, including thermal and electrical fixing[4−6], were developed to overcome volatility, but such techniques present practical disadvantages. Rapid optical refreshment of memory is also impossible. To solve this problem, Buse *et al.* demonstrated a two-center holographic recording technique, in which a LiNbO$_3$:Fe:Mn crystal was used in an all-optical experimental setup; however, low recording sensitivity was the main disadvantage of the technique[6]. Many factors that influence the recording sensitivity $S$ of congruent LiNbO$_3$:Fe:Mn were theoretically and experimentally investigated[7−11]. Another all-optical solution is the one-color quasi-nonvolatile holographic recording technique[12], which realizes high asymmetry in grating buildup and readout erasure rates in reduced LiNbO$_3$:In:Fe crystal.

Near-stoichiometric LiNbO$_3$ crystals exhibit significantly improved photorefractive properties[13−16]. Two-color nonvolatile holography was achieved in singly Fe-doped and pure near-stoichiometric LiNbO$_3$ crystals[17−21], and the enhanced recording sensitivity $S$ of stoichiometric LiNbO$_3$:Cu:Ce was reported[22]. These experimental results indicate that intrinsic defects are instrumental in improving the photorefractive properties of LiNbO$_3$. The nonvolatile holographic performance of LiNbO$_3$:Fe:Mn crystal has been extensively studied[7−11], but to the best of our knowledge, the influence of Li$_2$O content on the nonvolatile holographic properties of the doubly doped crystal remains unclear. In the current work, we investigated the nonvolatile holographic properties of LiNbO$_3$:Fe:Mn crystals that have different Li$_2$O contents. An improved recording sensitiv-

ity $S'$ of 0.15 cm/J was achieved with near-stoichiometric LiNbO$_3$:Fe:Mn.

LiNbO$_3$:Fe:Mn crystals with different Li$_2$O contents were prepared. LiNbO$_3$:Fe:Mn single crystal was grown along the $z$ axis from a congruent melt (48.38-mol% Li$_2$O, 51.62-mol% Nb$_2$O$_5$; 0.075-wt.-% Fe$_2$O$_3$, 0.01-wt.-% MnO) by the Czochralski process. The as-grown crystals were then cut into $x$-oriented plates. The vapor transport equilibration technique was employed to obtain LiNbO$_3$:Fe:Mn crystals with different Li$_2$O contents[23]. The plates were treated in powder charges with Li$_2$O/Nb$_2$O$_5$ ratios that ranged from 48.4/51.6 to 49.8/50.2, and then polished to optical grade with a thickness of 0.85 mm. The composition of each crystal was characterized by measuring the width of 153-cm$^{-1}$ Raman lines[24]. The Li$_2$O content of each crystal is listed in Table 1. Theoretical and experimental results[7,8] show that the oxidization–reduction state of the crystals strongly affects the nonvolatile holographic properties of LiNbO$_3$:Fe:Mn. The nonvolatile holographic properties of all the crystals in their original states were measured firstly. After the experiments, all the original-state crystals were reduced in argon gas at 700 °C for 4 h. Reduction in argon gas was repeated at 700 °C for 2 h.

The nonvolatile experimental setup is schematically illustrated in Fig. 1. An A4000 Hg lamp was used as the UV sensitizing light (365-nm central wavelength; 60-mW/cm$^2$ light intensity). An extraordinarily polarized beam from the Nd:YAG 532 nm laser was split into two beams with a light intensity of 600 mW/cm$^2$. The two recording beams were made to intersect symmetrically with respect to the $x$ axis inside the crystal to ensure that the grating vector of the interference pattern was aligned parallel to the $c$ axis of the crystal. The external intersected angle between the two beams was 30°. The signal light was occasionally blocked a computer-controlled electronic shutter S2 during recording to enable the reference beam to read out the written hologram and trace the temporal development of the hologram. The diffracted beam located after the hologram and the transmitted reference light were detected using D1 and D2, respectively. The propagation direc-

tion of the grating beam was set parallel to the bisector of the two writing beams. The "on" and "off" states of the sensitizing and signal beams were controlled by shutters S1, S2, and S3. Electronic shutter S3 was placed in front of the detector. The "on" and "off" states of S1 and S2 were set out of phase with each other to prevent direct exposure of the detector to the transmitted signal beam.

Nonvolatile holographic storage was achieved in all the crystals. Figure 2 shows the experimental results for $LN_{48.36}$:Fe:Mn. Diffraction efficiency $\eta$ is defined as $I_d/(I_d+I_t)$, where $I_d$ and $I_t$ are the diffracted and transmitted intensities of the reference beam, respectively. The figure also shows that during fixing, diffraction efficiency $\eta$ initially decreased to almost 50% in a short period before stabilizing. As a result, all gratings that were recorded on the shallow centers were totally erased and only those that were recorded on the deep centers remained.

Photorefractive sensitivity $S$ is the key index that describes how fast a hologram can be recorded at a fixed light intensity and material thickness. For two-color holography, given the partial erasure during the fixing process, the expression of $S$ was modified to $S' = \beta * (1/I_{rec}L)(\partial\sqrt{\eta}/\partial t)_{|t=0}$, where $\beta$ is the ratio of $\sqrt{\eta}$ after fixing and before fixing[9]. The $S'$ of all the crystals in different states are shown in Fig. 3. Sensitivity was highest after the first reduction, with sensitivity $S'$ reaching its maximum when $N_A \approx (0.8$–$0.9)N_{Mn}$ ($N_{A,S}$ the initial electron concentration in the Mn traps)[10]. For the original-state crystals, most of the traps were empty; thus, only a very weak hologram could be recorded. After the first reduction process, $N_A$ reached its optimum value and about 80% to 90% of the Mn traps were initially filled by electrons. After the second reduction process, more than 90% of the Mn traps were initially filled by electrons. Even though a very strong hologram could be recorded in this case, the majority of the hologram was destructive (i.e., $\beta$ with a very small value). The experimental results show that the reduction of the original-state crystal during the first 4 h improved sensitivity, but further reduction visibly decreased sensitivity.

The experimental results for the two-color nonvolatile holography of saturation diffraction efficiency $\eta_s$, fixing diffraction efficiency $\eta_f$, photorefractive sensitivity $S$, and the $S'$ of all the crystals after the first reduction are listed in Table 1.

The relationship among $\eta_s$, $S'$, and $Li_2O$ content is depicted in Fig. 4. Two key indexes were improved by increasing $Li_2O$ content, and the maximum values of $\eta_s$, $S'$, that is, 35.42% and 0.15 cm/J, were simultaneously
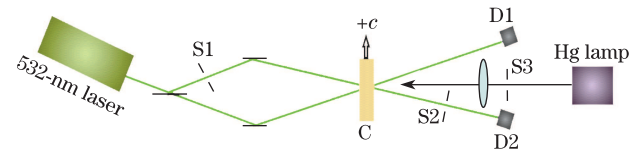


Fig. 1. Experimental setup for two-color nonvolatile holographic storage. BS: beam splitter; M1-M2: mirrors; S1-S3: electronic shutters; D1-D2: detectors; L: lens; C: crystal.
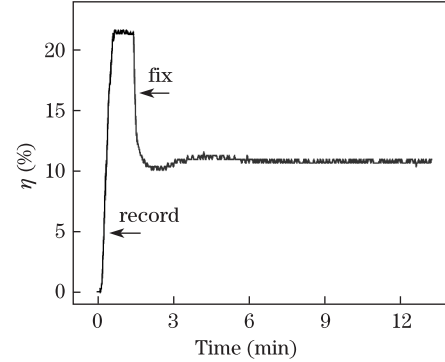


Fig. 2. Nonvolatile holographic performance of $LN_{48.4}$:Fe:Mn.
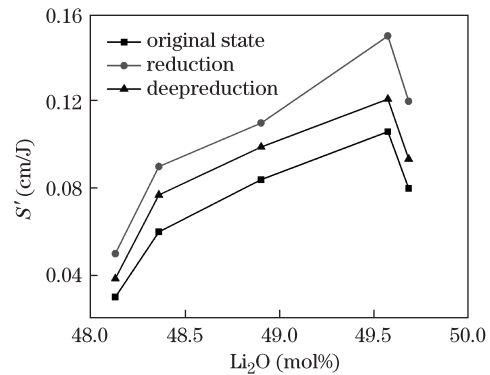


Fig. 3. Relationship between $S'$ and $Li_2O$ contents in $LiNbO_3$:Fe:Mn of different oxidization-reduction states.

achieved in $LN_{49.6}$:Fe:Mn. However, the further increase in $Li_2O$ content decreased photorefractive sensitivity $S'$. The improved nonvolatile holography properties of near-stoichiometric $LN_{49.6}$:Cu:Ce were reported in Ref. [22], and the optimal $Li_2O$ content in $LiNbO_3$:Cu:Ce coincides with that derived in the current work.

For two-center nonvolatile holographic recording in $LiNbO_3$:Fe:Mn crystal, saturation diffraction efficiency $\eta_s$ is determined according to the amount of electrons on the shallow centers, and recording sensitivity $S'$ depends

**Table 1. Values of Compositions $S$, $S'$, $\eta_s$, and $\eta_f$ of All the Crystals**

| Sample | $LN_{48.1}$:Fe:Mn | $LN_{48.4}$:Fe:Mn | $LN_{48.8}$:Fe:Mn | $LN_{49.6}$:Fe:Mn | $LN_{49.7}$Fe:Mn |
|---|---|---|---|---|---|
| Composition ($Li_2O$ mol%) | 48.1 | 48.4 | 48.8 | 49.6 | 49.7 |
| Recording $S$ (cm/J) | 0.10 | 0.13 | 0.19 | 0.23 | 0.18 |
| $S'$ (cm/J) | 0.05 | 0.09 | 0.11 | 0.15 | 0.12 |
| $\eta_s$ (%) | 17.42 | 21.38 | 25.27 | 35.42 | 30.46 |
| $\eta_f$ (%) | 4.34 | 10.96 | 11.47 | 15.05 | 13.54 |
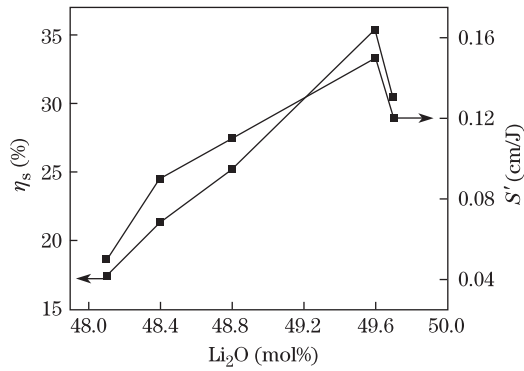
Fig. 4. Relationship among $\eta_s$, $S'$, and $Li_2O$ contents in $LiNbO_3$:Fe:Mn crystal.

primarily on the speed of electrons that are excited from the deep centers to the shallow centers. Ultraviolet light-induced absorption (ULIA) and bleaching experiment clearly characterize the charge transport process[9] during the recording process in two-center nonvolatile holography. Our previous ULIA experimental results[24] show that with increasing $Li_2O$ content, the saturation value of $\Delta\alpha$ increased and reached its maximum at 49.6 mol% $Li_2O$ content; this value then began to decline. The results of the bleaching experiment[25] agree with those for ultraviolet (UV) light-induced absorption; these two sets of experimental results indicate that the optimum $Li_2O$ content for two-color $LiNbO_3$:Fe:Mn holography should be about 49.6 mol%.

For both congruent LiNbO3:Fe:Mn and near-stoichiometric LiNbO3:Fe:Mn, Fe and Mn ions are the doped photorefractive shallow and deep centers in non-volatile holographic storage, respectively. Compared with congruent crystal, however, near-stoichiometric $LiNbO_3$:Fe:Mn has additional photorefractive centers ($Nb_{Li}^{4+}$:$Nb_{Nb}^{4+}$/$Nb_{Li}^{4+}$), except for the $Fe^{2+/3+}$ and $Mn^{2+/3+}$ doped photorefractive centers. The non-stoichiometric growth of $LiNbO_3$:Fe:Mn crystal enables intrinsic defects to function as photorefractive centers during nonvolatile holographic storage under certain conditions. Non-stoichiometric $LiNbO_3$ crystals exhibit numerous intrinsic defects, such as Li site vacancies ($V_{Li}^-$) and charge-compensated antisite Nb ($Nb_{Li}^{5+}$) ions. Some $Nb_{Li}^{5+}$ ions trap electrons and form small polarons ($Nb_{Li}^{4+}$) with a binding energy of 1.6 eV, and some $Nb_{Li}^{5+}$ together with neighboring normal site $Nb_{Nb}^{5+}$ trap a pair of electrons and become bipolarons ($Nb_{Li}^{4+}$:$Nb_{Nb}^{4+}$) with a binding energy of 2.5 eV[18]. With increasing $Li_2O$ content, the lifetime and amount of bipolarons and small polarons increase. An important consideration is that small polarons and bipolarons can reciprocally transform through illumination under a suitable wavelength light or by heat treatment[26]. Therefore, these two kinds of polarons can serve as intrinsic photorefractive centers for the $LiNbO_3$:Fe:Mn nonvolatile holographic experiment; it may also improve nonvolatile holographic storage properties. Hesselink et al.[18] successfully achieved nonvolatile holography in stoichiometric pure $LiNbO_3$ crystal by employing these two kinds of polarons as shallow and deep photorefractive centers. Yan et al.[27] reported that different defects dominate the photorefrac-

tive centers of pure $LiNbO_3$ with different $Li_2O$ contents, and that bipolarons are considered responsible for the enhanced photorefractive properties in near-stoichiometric $LiNbO_3$. In our previous work[22], the improved sensitivity of near-stoichiometric $LiNbO_3$:Cu:Ce contributed to the increase in bipolarons. Thus, the improved recording sensitivity $S'$ of near-stoichiometric $LiNbO_3$:Fe:Mn in the current study can also be ascribed to bipolarons. Herein, recording sensitivity $S'$ reached its maximum at a $Li_2O$ content of 49.6 mol%, and began to decrease at a $Li_2O$ content of 49.7 mol%. $LiNbO_3$:Fe:Mn and $LiNbO_3$:Cu:Ce have the same optimum $Li_2O$ content, and the result agrees with that in Ref. [18]. All the experimental results imply that for nonvolatile holographic storage, a bipolaron/small polaron is another photorefractive center that is crucial in improving nonvolatile holographic properties. At an appropriate $Li_2O$ content in the crystal, the amount and lifetime of bipolarons increase.

In conclusion, nonvolatile holographic storage is realized in near-stoichiometric $LiNbO_3$:Fe:Mn crystals. The influence of $Li_2O$ content on nonvolatile holographic properties of $LiNbO_3$:Fe:Mn is investigated in detail. Increasing $Li_2O$ content in $LiNbO_3$:Fe:Mn is favorable for improving recording sensitivity and diffraction efficiency. The optimum $Li_2O$ content is about 49.6 mol%.

References

1. D. Psaltis and F. Mok, Sci. Am. **273,** 70 (1995).
2. M. Lee, S. Takekawa, Y. Furukawa, K. Kitamura, and H. Hatano, Phys. Rev. Lett. **84,** 875 (2000).
3. L. Dhar, K. Curtis, and T. Fäcke, Nat. Photon. **2,** 403 (2008).
4. J. J. Amodei and D. L. Staebler, Appl. Phys. Lett. **18,** 540 (1971).
5. F. Micheron and G. Bismuth, Appl. Phys. Lett. **20,** 79 (1972).
6. K. Buse, A. Adibi, and D. Psaltis, Nature **393,** 665 (1998).
7. Y. Liu, L. Liu, and C. Zhou, Opt. Lett. **25,** 551 (2000).
8. A. Adibi, K. Buse, and D. Psaltis, Appl. Phys. Lett. **74,** 3767 (1999).
8. A. Adibi, K. Buse, and D. Psaltis, Opt. Lett. **15,** 539 (2000).
10. O. Momtahan and A. Adibi, J. Opt. Soc. Am. B **20,** 449 (2003).
11. O. Momtahan, A. Makhmalbaf, and A. Adibi, Appl. Phys. B **90,** 519 (2008).
12. G. Zhang , Y. Tomita, X. Zhang, and J. Xu, Appl. Phys. Lett. **81,** 1393 (2002).
13. T. Zhang, B. Wang, S. Fang, and D. Ma, J. Phys. D **38,** 2013 (2005).
14. K. Kitamura, Y. Furukawa, Y. Ji, M. Zgonik, C. Medrano, G. Montemezzani, and P. Günter, J. Appl. Phys. **82,** 1006 (1996).
15. Y. Furukawa, K. Kitamura, Y. Ji, G. Montemezzani, M. Zgonik, C. Medrano, and P. Günter, Opt. Lett. **22,** 501 (1997).
16. H. Liu, X. Xie, Y. Kong, W. Yan, X. Li, L. Shi, J. Xu,

and G. Zhang, Opt. Mater. **28,** 212 (2006).

17. Y. S. Bai and R. Kachru, Phys. Rev. Lett. **78,** 2944 (1997).

18. L. Hesselink, S. Orlov, A. Liu, A. Akella, D. Lande, and R. Neurgaonkar, Science **282,** 1089 (1998).

19. H. Guenther, R. Macfarlane, Y. Furukawa, K. Kitamura, and R. Neurgaonkar, Appl. Opt. **37,** 7611 (1998).

20. Y. Liu, K. Kitamura, S. Takekawa, M. Nakamura, Y. Furukawa, and H. Hatano, Appl. Phys. Lett. **82,** 4218 (2009).

21. S. Chen, X. Liu, B. Fu, and G. Zhang, Chin. Opt. Lett. **7,** 67 (2009).

22. X. Li, Y. Kong, Y. Wang, L. Wang, F. Liu, H. Liu, Y. An, S. Chen, and J. Xu, Appl. Opt. **46,** 7620 (2007).

23. P. F. Borbui, R. G. Norwood, D. H. Jundt, and M. M. Fejer, J. Appl. Phys. **71,** 875 (1992).

24. M. Wöhlecke, G. Corradi, and K. Betzler, Appl. Phys. B **63,** 323 (1996).

25. O. Schirmerm, O. Themann, and M. Wöehlecke, J. Phys. Chem. Solids **52,** 185 (1991).

26. H. J. Reyher, R. Schulz, and O. Thiemann, Phys. Rev. B **50,** 3609 (1994).

27. W. Yan, Y. Kong, L. Shi, L. Sun, H. Liu, X. Li, D. Zhao, and J. Xu, Appl. Opt. **45,** 2453 (2006).